STRESS-INTENSITY FACTORS FOR A WEDGE-LOADED EDGE CRACK IN A SEMI-INFINITE STRIP

by

F. Erdogan and H. Terada

(NASA-CR-145264) STRESS-INTENSITY FACTORS FOR A WEDGE-LOADED EDGE CRACK IN A SEMI-INFINITE STRIP (Lehigh Univ.) 32 p HC A03/MF A01 CSCL 20K

N78-10507

Unclas
G3/39 51857

July 1977

Lehigh University
Bethlehem, Pa.

THE NATIONAL AERONAUTICS AND SPACE ADMINISTRATION
GRANT NO. NGR 39-007-011

STRESS-INTENSITY FACTORS FOR A WEDGE-LOADED EDGE CRACK IN A SEMI-INFINITE STRIP

by

F. Erdogan and H. Terada

July 1977

Lehigh University
Bethlehem, Pa.

THE NATIONAL AERONAUTICS AND SPACE ADMINISTRATION
GRANT NO. NGR 39-007-011

STRESS-INTENSITY FACTORS FOR A WEDGE-LOADED EDGE CRACK IN A SEMI-INFINITE STRIP*

by

F. Erdogan and H. Terada**
Lehigh University, Bethlehem, Pa.

ABSTRACT

The problem of a semi-infinite strip containing an edge crack is considered. It is assumed that the strip is loaded by a frictionless rigid wedge pressed into the crack. The resulting crack-contact problem is formulated in terms of a system of singular integral equations. The behavior of the solution near the singular points is studied in detail. A series of numerical examples are given and the results are compared with those obtained by the method of boundary collocation and by the simple beam theory.

1. Introduction

Wedge loading of elastic materials is used in practice mainly in certain fracture toughness characterization tests and in fracturing solids by wedge-splitting or cleaving. In the former case the geometry of the medium is usually a rectangular strip which contains a symmetric edge crack. The specimen is known as the "compact tension specimen" if the length of the strip is of the same order of magnitude as its height, and as the "trousers' legs specimen" if its length is very long compared to its height. In fracturing of solids there is, of course, no standard geometry. However, in this case too a traction-free surface, an edge crack, and a bounded geometry with a rigid wedge pressed into the crack may be considered as the distinct features of the related solid mechanics problem. In solving these problems it is generally assumed that the external load is either a concentrated wedge force or is distributed in

---

*This work was supported by NASA-Langley under the Grant NGR 39-007-011 and by NSF under the Grant ENG 77-19127.

**Permanent address: National Aerospace Laboratory, 1880 Jindaiji Chofu, Tokyo, Japan.

some known fashion (see, for example, [1] and [2]). However, if the load is applied to the solid by pressing a rigid wedge into the crack, the problem is clearly a crack-contact problem in which the contact stresses and in some cases the contact area are additional unknowns.

There are a number of solutions available in which the stress intensity factor is evaluated in the compact tension specimen and in the semi-infinite strip for various types of traction boundary conditions [1-4]. However, the related contact-crack problem which is described in Figure 1a does not seem to have been considered before. The contact problems considered in [5] and [6] discuss the wedging of infinite solids containing a V-notch prior to the formation of cracks. In this paper the wedge loading problem for a semi-infinite strip shown in Figure 1a is considered. The previous solutions for this geometry were based, in one form or another, on either a boundary collocation technique [1-3] or finite element methods (see, for example, [4] for a review). Here the elasticity problem is formulated in terms of a system of integral equations and the contact stresses and the stress intensity factor is obtained for various loading conditions.

2. Formulation

To formulate the problem first the infinite strip containing three symmetric cracks and shown in Figure 1b is considered. It is seen that the formulation of the desired problem shown in Figure 1a may be obtained from that of Figure 1b by letting $d \to h$ and $c \to 0$. In this study it is assumed that the wedge is rigid and the contact is frictionless. Thus, the problem is symmetric with respect to x and y axes in geometry as well as in loading. Consequently it is sufficient to consider one fourth of the region only (i.e., $0<x<\infty$ and $0<y<h$). In this region the x and y-components of the displacement vector satisfying the related equilibrium equations, the regularity conditions at $x=\infty$, and the boundary condition of zero shear traction on $x=0$, $0<y<h$ (i.e., $\sigma_{xy}(0,y)=0$) may be expressed as follows [7,8]:

$$u(x,y) = \frac{2}{\pi}\int_0^\infty \{\frac{1}{s}(f_1 + \frac{\kappa+1}{2} g_1 + syg_2)\sinh(sy)$$

$$+ \frac{1}{s}(f_2 + \frac{\kappa+1}{2} g_2 + syg_1)\cosh(sy)\}\sin(sx)dx$$

$$+ \frac{1}{2\pi}\int_{-\infty}^{\infty}(\frac{\kappa+1}{2} + |s|x)g_3 e^{-|s|x + isy} ds \quad , \tag{1}$$

$$v(x,y) = -\frac{2}{\pi}\int_0^\infty \{\frac{1}{s}(f_2 - \frac{\kappa-1}{2} g_2 + syg_1)\sinh(sy)$$

$$+ \frac{1}{s}(f_1 - \frac{\kappa-1}{2} g_1 + syg_2)\cosh(sy)\}\cos(sx)ds$$

$$+ \frac{i}{2\pi}\int_{-\infty}^{\infty}(\frac{\kappa-1}{2}\frac{|s|}{s} - sx)g_3 e^{-|s|x + isy} ds \tag{2}$$

where κ is the elastic constant ($\kappa = 3-4\nu$ for plane strain, i.e., for $B>>h$, and $\kappa = (3-\nu)/(1+\nu)$ for generalized plane stress, i.e., for $B<<h$, B being the thickness of the strip), and f_1, f_2, g_1, g_2, and g_3 are unknown and are functions of s. These unknowns are determined by the remaining boundary conditions which may be expressed as

$$\sigma_{yy}(x,h) = 0 \quad , \quad \sigma_{xy}(x,h) = 0 \quad , \quad 0<x<\infty \quad , \tag{3a,b}$$

$$\sigma_{xy}(x,0) = 0 \quad , \quad 0<x<\infty \quad , \tag{4}$$

$$\left.\begin{array}{l} \sigma_{xx}(0,y) = 0 \quad , \quad c<y<d \quad , \\ u(0,y) = 0 \quad , \quad 0<y<c \quad , \quad d<y<h \quad , \end{array}\right\} \tag{5}$$

$$\left.\begin{array}{l} \sigma_{yy}(x,0) = 0 \quad , \quad 0\le x<a_0 \quad , \quad a<x<b \quad , \\ \frac{\partial}{\partial x} v(x,0) = f(x) \quad , \quad a_0<x<a \quad , \\ \frac{\partial}{\partial x} v(x,0) = 0 \quad , \quad b<x<\infty \end{array}\right\} \tag{6}$$

Three homogeneous conditions (3) and (4) may be used to eliminate three of the unknown functions. The mixed boundary conditions (5) and (6) give a system of two dual integral equations to determine the remaining two functions. To obtain the relevant integral equations of the problem in this paper, however, a more direct method is used by defining the following two new unknown functions:

$$\frac{\partial}{\partial y} u(0,y) = \phi(y) \quad , \quad c<y<d \quad , \tag{7}$$

$$\frac{\partial}{\partial x} v(x,0) = \psi(x) \quad , \quad 0\leq x<b \quad . \tag{8}$$

Note that outside the domains indicated in (7) and (8) the functions $\phi(y)$ and $\psi(x)$ are zero. Thus, differentiating (1), letting $x=0$, and inverting, g_3 may be expressed in terms of ϕ. After eliminating three of the remaining four unknowns by using (3) and (4) and the stress-displacement relations, the last unknown function may be expressed in terms ϕ and ψ by again differentiating and inverting equation (2). After some straightforward manipulations the stress components involved in the mixed boundary conditions (5) and (6) may be expressed as

$$\pi \frac{1+\kappa}{4\mu} \sigma_{xx}(0,y) = \int_c^d H_{11}(y,r)\phi(r)dr$$

$$+ \int_0^b H_{12}(y,t)\psi(t)dt \quad , \quad c<y<d \quad , \tag{9}$$

$$\pi \frac{1+\kappa}{4\mu} \sigma_{yy}(x,0) = \int_c^d H_{21}(x,r)\phi(r)dr$$

$$+ \int_0^b H_{22}(x,t)\psi(t)dt \quad , \quad 0<x<b \quad , \tag{10}$$

where μ is the shear modulus, and the kernels H_{ij}, $(i,j=1,2)$ are found to be

$$H_{11}(y,r) = \frac{1}{r-y} + \frac{1}{r+y} + h_{11}(y,r) - h_{11}(y,-r) \quad , \tag{11a}$$

$$h_{11}(y,r) = \int_0^\infty \frac{A_1\cosh(ys) + A_2\sinh(ys)}{1 + 4she^{-2sh} - e^{-4sh}}\, ds \quad , \tag{11b}$$

$$A_1(s) = 2e^{-(2h-r)s}(-2s^2h^2 + 2s^2rh - 3sr$$

$$- sre^{-2sh} + 4sh - 2 - 2e^{-2sh}) \quad , \tag{11c}$$

$$A_2(s) = -2sye^{-(2h-r)s}(1 - 2sh + 2sr + e^{-2sh}) \quad , \tag{11d}$$

$$H_{12}(y,t) = \frac{2t(t^2-y^2)}{(y^2+t^2)^2} - 2\int_0^\infty \frac{B_1\cosh(ys) + B_2\sinh(ys)}{1 + 4she^{-2sh} - e^{-4sh}} \sin(ts) ds \quad , \tag{12a}$$

$$B_1(s) = e^{-2sh}(1 + 2hs - 2h^2s^2 - e^{-2hs}) \quad , \tag{12b}$$

$$B_2(s) = e^{-2hs}ys(1 + 2hs - e^{-2hs}) \quad , \tag{12c}$$

$$H_{21}(x,r) = \frac{2r(r^2-x^2)}{(x^2+r^2)^2} + 2\int_0^\infty \frac{C\cos(sx)\,ds}{1 + 4hse^{-2hs}e^{-4hs}} \quad , \tag{13a}$$

$$C(s) = e^{-2hs}[e^{sr}(2h^2s^2 - 2hs^2r - sr + sre^{-2hs})$$

$$- e^{-sr}(2h^2s^2 + 2hs^2r + sr - sre^{-2hs})] \quad , \tag{13b}$$

$$H_{22}(x,t) = \frac{1}{t-x} + \frac{1}{t+x} + h_{22}(x,t) \quad , \tag{14a}$$

$$h_{22}(x,t) = 2\int_0^\infty \frac{e^{-2hs}(e^{-2hs} - 2h^2s^2 - 2hs - 1)}{1 + 4hse^{-2hs} - e^{-4hs}} [\sin s(t-x)$$

$$+ \sin s(t+x)\Big]ds \quad . \tag{14b}$$

For c>0 and d<h it can be shown that the kernels h_{11}, H_{12}, H_{21}, and h_{22} are bounded within the rectangular closed intervals in which they are defined. In this case, referring to Figure 1b, the definitions (7) and (8), and the mixed boundary conditions (5) and (6), it may be seen that the unknown functions ϕ and ψ must satisfy the following conditions of single-valuedness of displacements:

$$\int_c^d \phi(y)dy = 0 \quad , \tag{15}$$

$$\int_{-b}^{b} \psi(x)dx = 0 \quad . \tag{16}$$

Even though this problem is not very practical, it can be solved without any difficulty. For example, if in addition to wedging, the strip is subjected to a uniform stress $\sigma_{xx}(\mp\infty,y) = \sigma_o$, the integral equations (9) and (10) may be expressed as

$$\int_c^d H_{11}(y,r)\phi(r)dr + \int_0^{a_o} H_{12}(y,t)\psi_1(t)dt + \int_a^b H_{12}(y,t)\psi_2(t)dt$$

$$= - \pi \frac{1+\kappa}{4\mu} \sigma_o - \int_{a_o}^a H_{12}(y,t)f(t)dt \quad , \quad c<y<d \quad , \tag{17}$$

$$\int_c^d H_{21}(x,r)\phi(r)dr + \int_0^{a_o} H_{22}(x,t)\psi_1(t)dt + \int_a^b H_{22}(x,t)\psi_2(t)dt$$

$$= - \int_{a_o}^a H_{22}(x,t)f(t)dt \quad , \quad 0<x<a_o \quad , \tag{18}$$

$$\int_c^d H_{21}(x,r)\phi(r)dr + \int_0^{a_o} H_{22}(x,t)\psi_1(t)dt + \int_a^b H_{22}(x,t)\psi_2(t)dt$$

$$= - \int_{a_o}^a H_{22}(x,t)f(t)dt \quad , \quad a<x<b \quad , \tag{19}$$

where it is assumed that

$$\frac{\partial}{\partial x} v(x,0) = \psi(x) = \begin{cases} \psi_1(x) & , \quad 0<x<a_0 \quad , \\ f(x) & , \quad a_0<x<a \quad , \\ \psi_2(x) & , \quad a<x<b \quad , \end{cases} \tag{20}$$

and $f(x)$ is known from the wedge profile. The unknown functions ϕ, ψ_1, and ψ_2 are obtained from the system of singular integral equations (17-19) in which only the main diagonal terms in the kernel matrix contain Cauchy singularities. For the integral equations defined on a union of arcs this scheme of increasing the number of the unknown functions and integral equations in such a way that each equation is defined on a single arc makes it possible to solve the system numerically in a straightforward fashion. Otherwise, due to the complicated nature of the related fundamental functions, it would have been difficult and quite cumbersome to obtain a numerical solution. The index of (17) is +1 and the conditon (15) is still valid. The indexes of (18) and (19) and the corresponding additional conditions depend on the wedge profile.

3. The End Problem

If we let $d = h$ and $c = 0$ the problem becomes a stress-free "end problem". In this case it can be shown that for $y = h = r$ the kernel h_{11} given by (11b) is not bounded. To show this and to separate the singular part of this kernel consider the leading exponential terms in $A_1(s)$ and $A_2(s)$, which may be written as

$$A_{1\infty}(s) = 2e^{-(2h-r)s}(-2s^2h^2 + 2s^2rh - 3sr + 4sh - 2) \quad ,$$

$$A_{2\infty}(s) = -2sye^{-(2h-r)s}(1 - 2sh + 2sr) \quad . \tag{21a,b}$$

By adding and subtracting $A_{1\infty}$ and $A_{2\infty}$ under the integral in (11b) and by using the relation [10]

$$\int_0^\infty s^m e^{(2h-r)s} \begin{Bmatrix} \sinh(sy) \\ \cosh(sy) \end{Bmatrix} ds = \frac{d^m}{dr^m} \int_0^\infty e^{-(2h-r)s} \begin{Bmatrix} \sinh(sy) \\ \cosh(sy) \end{Bmatrix} ds$$

$$= \frac{d^m}{dr^m} \left[\frac{1}{(2h-r)^2-y^2} \begin{Bmatrix} y \\ 2h-r \end{Bmatrix} \right] , \tag{22}$$

the kernel $h_{11}(y,r)$ may easily be expressed as follows:

$$h_{11}(y,r) = h_s(y,r) + h_b(y,r) , \tag{23}$$

$$h_s(y,r) = \frac{1}{2h-y-r} + \frac{6(h-y)}{(2h-y-r)^2} + \frac{4(h-y)^2}{(2h-r-y)^3} ,$$

$$= [-1 + 6(h-y) \frac{d}{dy} - 2(h-y)^2 \frac{d^2}{dy^2}] \frac{1}{r-(2h-y)} , \tag{24}$$

$$h_b(y,r) = \int_0^\infty \{[\frac{A_1(s)}{1+ 4she^{-2sh} - e^{-4sh}} - A_{1\infty}(s)]\cosh(ys)$$

$$+ [\frac{A_2(s)}{1+ 4she^{-2sh} - e^{-4sh}} - A_{2\infty}(s)]\sinh(ys)\}ds . \tag{25}$$

The kernel h_b is bounded in $0 \le (y,r) \le h$ and the singular part h_s together with the singular terms $1/(r-y)$ and $1/(r+y)$ in (11a) constitute a generalized Cauchy kernel.

To investigate the behavior of the solution of (9) and (10) at the end points $(x = 0,\ y = h)$ and $(x = 0,\ y = 0)$ let

$$\phi(r) = \frac{f(r)}{r^\alpha(h-r)^\beta} = \frac{f(r)e^{\pi i\beta}}{r^\alpha(r-h)^\beta} , \quad 0<r<h , \tag{26}$$

$$\psi(t) = \frac{g(t)}{t^\alpha(b-t)^\gamma} = \frac{g(t)e^{\pi i\gamma}}{t^\alpha(t-b)^\gamma} , \quad 0<t<b , \tag{27}$$

where f is Hölder-continuous in $0<r<h$, $r^\alpha(r-h)^\beta$ is a definite branch varying continuously in $0<r<h$, and it is assumed that

$$f(0) \neq 0 \quad , \quad f(h) \neq 0 \quad , \quad 0 < Re(\alpha,\beta) < 1 \quad . \tag{28}$$

Similar statements hold for $g(t)$. At the common end point $(r = 0,\ t = 0)$ the functions ϕ and ψ must have the same singular behavior, hence the common power α in (26) and (27). Define now the following sectionally holomorphic functions:

$$F(z_1) = \frac{1}{\pi}\int_0^h \frac{\phi(r)}{r-z_1}\,dr \quad , \quad G(z_2) = \frac{1}{\pi}\int_0^b \frac{\psi(t)}{t-z_2}\,dt \quad , \tag{29a,b}$$

where the variables y and r are on the line $Re(z_1)$ and x and t are on $Re(z_2)$. Analyzing the asymptotic behavior of, for example, $F_1(z)$ around the end points $z_1 = 0$ and $z_1 = h$ by following the procedure described in [11], we obtain

$$F(z_1) = \frac{f(0)e^{\pi i\alpha}}{h^{\beta}\sin\pi\alpha}\,\frac{1}{z_1^{\alpha}} - \frac{f(h)}{h^{\alpha}\sin\pi\beta}\,\frac{1}{(z_1-h)^{\beta}} + F_o(z_1) \quad , \tag{30}$$

$$\frac{1}{\pi}\int_0^h \frac{\phi(r)}{r-y}\,dr = \frac{f(0)\cot\pi\alpha}{h^{\beta}}\,\frac{1}{y^{\alpha}} - \frac{f(h)\cot\pi\beta}{h^{\alpha}}\,\frac{1}{(h-y)^{\beta}} + F_1(y) \quad , \tag{31}$$

$$\frac{1}{\pi}\int_0^h \frac{\phi(r)}{r+y}\,dr = F(-y) = \frac{f(0)}{h^{\beta}\sin\pi\alpha}\,\frac{1}{y^{\alpha}} + F_2(y) \quad , \tag{32}$$

$$\frac{1}{\pi}\int_0^h \frac{\phi(r)dr}{r-(2h-y)} = F(2h-y) = -\frac{f(h)}{h^{\alpha}\sin\pi\beta}\,\frac{1}{(h-y)^{\beta}} + F_3(y) \quad , . \tag{33}$$

where the functions F_j, $(j = 0,..,3)$ are bounded everywhere with possible exceptions of the ends o and h where they may have singularities weaker than $z_1^{-\alpha}$ and $(z_1-h)^{-\beta}$, respectively. The remaining two terms coming from (24) may be obtained from (33) by differentiation. Similarly

$$G(z_2) = \frac{g(0)e^{\pi i\alpha}}{b^{\gamma}\sin\pi\alpha}\,\frac{1}{z_2^{\alpha}} - \frac{g(b)}{b^{\alpha}\sin\pi\gamma}\,\frac{1}{(z_2-b)^{\gamma}} + G_o(z_2) \quad , \tag{34}$$

$$\frac{1}{\pi}\int_0^b \frac{\psi(t)}{t-x}\,dt = \frac{g(0)\cot\pi\alpha}{b^\gamma}\frac{1}{x^\alpha} - \frac{g(b)\cot\pi\gamma}{b^\alpha}\frac{1}{(b-x)^\gamma} + G_1(x) \quad , \tag{35}$$

$$\frac{1}{\pi}\int_0^b \frac{\psi(t)}{t+x}\,dt = G(-x) = \frac{g(0)}{b^\gamma \sin\pi\alpha}\frac{1}{x^\alpha} + G_2(x) \quad , \tag{36}$$

where G_o, G_1, and G_2 are again either bounded or have weaker end singularities.

Consider now the singular kernels in H_{12} and H_{21} given in (12a) and (13a). Note that these kernels are identical and may be expressed as

$$2\,\frac{t(t^2-y^2)}{(t^2+y^2)^2} = \frac{2t}{t^2+y^2} + 2y\,\frac{d}{dy}\left(\frac{t}{t^2+y^2}\right) \tag{37}$$

Now, observing that

$$\frac{2t}{t^2+y^2} = \frac{1}{t-iy} + \frac{1}{t+iy} \quad ,$$

and at $z_2 = \mp\, iy$ G is holomorphic, we obtain

$$\frac{1}{\pi}\int_0^b \frac{2t}{t^2+y^2}\,\psi(t)dt = G(iy) + G(-iy)$$

$$= \frac{2g(0)\cos(\pi\alpha/2)}{b^\gamma \sin\pi\alpha}\frac{1}{y^\alpha} + G_3(y) \quad , \tag{38}$$

$$y\,\frac{d}{dy}\,\frac{1}{\pi}\int_0^b \frac{2t}{(t^2+y^2)^2}\,\psi(t)dt = -\,\frac{2g(0)\cos(\pi\alpha/2)}{b^\gamma \sin\pi\alpha}\,\frac{\alpha}{y^\alpha} + G_4(y) \quad , \tag{39}$$

where, again at $y = 0$ G_3 and G_4 are either bounded or have singularitites weaker than $y^{-\alpha}$. Similarly

$$\frac{2}{\pi}\int_0^h \frac{r(r^2-x^2)}{(r^2+x^2)^2}\,\phi(r)dr = \frac{2f(0)\cos(\pi\alpha/2)}{h^\beta \sin\pi\alpha}\,\frac{1-\alpha}{x^\alpha} + F_4(x) \quad . \tag{40}$$

Note that in $0 \le y \le h$ $\sigma_{xx}(0,y)$ is bounded and with ϕ and ψ as defined in (26) and (27), the integrals involving the Fredholm kernels in (9) and (10) contribute only bounded terms. Thus, substituting from (31), (32), (33), (24), (38), and (39) into (9), multiplying both sides first by $(h-y)^{\beta}$ and letting $y \to h$, and then by y^{α} and letting $y \to 0$, we obtain the following relations:

$$\frac{f(h)}{h^{\alpha}\sin\pi\beta}\,[2(1-\beta)^2 - (1+\cos\pi\beta)] = 0 \quad , \tag{41}$$

$$\frac{f(0)}{h^{\beta}}\,(\cot\pi\alpha + \frac{1}{\sin\pi\alpha}) + \frac{g(0)}{b^{\gamma}}\,2(1-\alpha)\,\frac{\cos(\pi\alpha/2)}{\sin\pi\alpha} = 0 \quad . \tag{42}$$

The characteristic equation (41) giving β is identical to that of edge crack and 90-degree infinite elastic wedge [8]. Note that (41) has no root in the strip $0<\mathrm{Re}(\beta)<1$. Hence the function $\phi(r)$ has no power singularity at $r=h$.

Similarly, substituting from (40), (35), and (36) into (10) we obtain

$$\frac{g(b)}{b^{\alpha}}\cot\pi\gamma = 0 \quad , \tag{43}$$

$$\frac{f(0)}{h^{\beta}}\,2(1-\alpha)\,\frac{\cos(\pi\alpha/2)}{\sin\pi\alpha} + \frac{g(0)}{b^{\gamma}}\,(\cot\pi\alpha + \frac{1}{\sin\pi\alpha}) = 0 \quad . \tag{44}$$

Since $g(b) \neq 0$, (43) gives $\gamma = 1/2$ which is the standard value for an imbedded crack tip. Also since $f(0)$ and $g(0)$ are finite and unknown, (42) and (44) gives

$$\frac{1+\cos\pi\alpha}{\sin^2\pi\alpha}\,[(1 + \cos\pi\alpha) - 2(1-\alpha)^2] = 0 \quad . \tag{45}$$

As expected this is essentially the same characteristic equation obtained from (41) for the corner $(x=0,\ y=h)$. Hence, at the corner $(x=0,\ y=0)$ the functions $\phi(y)$ and $\psi(x)$ have no power singularity.

We can now proceed and show that $\phi(r)$ is a bounded function in the closed interval $0 \le r \le h$, and $\psi(t)$ has the following form

$$\psi(t) = \frac{g(t)}{(b-t)^{\gamma}} = \frac{g(t)e^{\pi i \gamma}}{(t-b)^{\gamma}} , \quad 0 \le t < b , \tag{46}$$

where g is bounded in $0 \le t \le b$. Starting with the definitions (29) the following asymptotic relations may be obtained [11]:

$$F(z_1) = -\frac{1}{\pi}\phi(0)\log z_1 + \frac{1}{\pi}\phi(h)\log(z_1-h) + C_0(z_1) , \tag{47}$$

$$\frac{1}{\pi}\int_0^h \frac{\phi(r)}{r-y}\,dr = -\frac{1}{\pi}\phi(0)\log y + \frac{1}{\pi}\phi(h)\log(y-h) + C_1(y) , \tag{48}$$

$$\frac{1}{\pi}\int_0^h \frac{\phi(r)}{r+y}\,dr = -\frac{1}{\pi}\phi(0)\log(-y) + C_2(y) , \tag{49}$$

$$G(z_2) = -\frac{1}{\pi}\frac{g(0)}{b^{\gamma}}\log z_2 - \frac{g(b)}{\sin\pi\gamma}\frac{1}{(z-b)^{\gamma}} + C_3(z_2) , \tag{50}$$

$$\frac{1}{\pi}\int_0^b \frac{\psi(t)}{t-x}\,dt = -\frac{1}{\pi}\frac{g(0)}{b^{\gamma}}\log x - g(b)\cot\pi\gamma \frac{1}{(b-x)^{\gamma}} + C_4(x) , \tag{51}$$

$$\frac{1}{\pi}\int_0^b \frac{2t}{t^2+y^2}\psi(t)dt = G(iy) + G(-iy) = -\frac{2}{\pi}\frac{g(0)}{b^{\gamma}}\log y + C_5(y) , \tag{52}$$

$$y\frac{1}{\pi}\frac{d}{dy}\int_0^b \frac{2t}{t^2+y^2}\psi(t)dt = C_6(y) , \tag{53}$$

$$\frac{1}{\pi}\int_0^h \frac{2r}{r^2+x^2}\phi(r)dr = -\frac{2}{\pi}\phi(0)\log x + C_7(x) , \tag{54}$$

$$\frac{1}{\pi}\int_0^b \frac{\psi(t)}{t+x}\,dt = -\frac{1}{\pi}\frac{g(0)}{b^{\gamma}}\log(-x) + C_8(x) , \tag{55}$$

where $C_0,..,C_8$ are bounded functions.

In equations (9) and (10) the left hand sides are bounded and the terms involving Fredholm kernels give finite quantities. Thus, substituting from (47)-(55) into (9) and (10), combining the finite quantities, and observing that $\log(-z) = \log z + \pi i$, we obtain

$$- \frac{2}{\pi} [\phi(0) + \frac{g(0)}{b^{\gamma}}] \log y + \frac{1}{\pi} \phi(h)[\log(y-h) - \log(h-y)]$$

$$+ C_9(y) = C_{10}(y) \quad , \tag{56}$$

$$- \frac{2}{\pi} [\phi(0) + \frac{g(0)}{b^{\gamma}}] \log x - g(b) \cot\pi\gamma \frac{1}{(b-x)^{\gamma}} + C_{11}(x) = C_{12}(x) \quad , \tag{57}$$

where $C_9, \ldots, C_{12}$ are bounded functions. Since $g(b)$ is finite (57) gives $\cot\pi\gamma = 0$, and $\gamma = 1/2$, which is the standard result. The logarithmic terms in the second term of (56) cancel. For the remaining unbounded terms involving $\log y$ and $\log x$ to vanish we must impose the following condition:

$$\phi(0) + \frac{g(0)}{b^{\gamma}} = 0 \quad . \tag{58}$$

Of course, (58) is nothing but the statement of the physical condition that, in the absence of shear tractions, after deformations there is no change in the 90-degree angle at $(x = 0, y = 0)$. This follows from

$$\phi(y) = \frac{\partial}{\partial y} u(+0,y) \quad , \quad \psi(x) = \frac{\partial}{\partial x} v(x,+0) = \frac{g(x)}{(b-x)^{\gamma}} \quad . \tag{59}$$

In solving the integral equations for the free corner problem with ϕ and ψ as the unknown functions (i.e., for $a_0 > 0$, $c = 0$ in Figure 1), (58) must be used as an additional condition.

Referring to Figure 1 if $a_0 = 0$, around the end point $x = 0$, $y = 0$, the function $\psi(x)$ is known and, since the wedge if frictionless, the contact stress is a bounded normal traction. Therefore, the analyses given in this section, including the condition (58) regarding the behavior of $\phi(y)$ remain to be valid.

4. Examples

As a first example consider the (frictionless) wedging problem shown in the insert of Figure 2 where it is assumed that $c = 0$, $d = h$, and the wedge is "flat", i.e.,

$$\frac{\partial}{\partial x} v(x,0) = f(x) = 0 \quad , \quad 0<x<a \quad . \tag{60}$$

Referring to Figure 1b, it is also assumed that $a_0 = 0$. This assumption is, of course, subject to the verification that in the region ($0<x<a$, $y = 0$) the contact stress $\sigma_{yy}(x,0)$ is compressive. In this problem the tractions on the crack surface are zero, the external load is provided by the wedge which has a total thickness $2v_0$, and the integral equations (9) and (10) are still valid and may be expressed in the form (see equations (9) and (10))

$$\int_0^h H_{11}(y,r)\phi(r)dr + \int_a^b H_{12}(y,t)\psi(t)dt = 0 \quad , \quad 0<y<h \quad , \tag{61}$$

$$\int_0^h H_{21}(x,r)\phi(r)dr + \int_a^b H_{22}(x,t)\psi(t)dt = 0 \quad , \quad a<x<b \quad . \tag{62}$$

The unknown function ϕ is bounded in $0\le y\le h$ and is zero at $y = 0$, whereas ψ has integrable (square root) singularities at $x = a$ and $x = b$. In solving the integral equations numerically it is assumed that

$$\psi(t) = G(t)[(t-a)(b-t)]^{-1/2} \quad , \quad a<t<b \quad , \tag{63}$$

where G is bounded in $a\le t\le b$. Thus the index of (62) is +1 and the solution is subject to the following additional condition

$$v(a,0) = v_0 = -\int_a^b \psi(t)dt \quad . \tag{64}$$

The integrals involving $\psi(t)$ may be evaluated by using the Gauss-Chebyshev integration formulas given in [9] after normalizing the interval (a,b) as

$$\xi = (2x-a-b)/(b-a) \quad , \quad \tau = (2t-a-b)/(b-a) \quad . \tag{65}$$

To evaluate the integrals involving $\phi(r)$ first the variables y and r are changed as

$$y = h - \eta \quad , \quad r = h - \rho \tag{66}$$

and then the definition of ϕ and the kernels are extended into $-h<\eta<0$, $-h<\rho<0$. By defining now

$$\phi(r) = \phi(h-\rho) = \phi_0(\rho) = g(\rho)[h^2-\rho^2]^{1/2} \quad , \tag{67}$$

the Gauss-Chebyshev integration formulas may then be used to evaluate the integrals [9,8].

After the density functions are obtained the stress intensity factor $k(b)$ at the crack tip and the strength of the compressive stress singularity $k(a)$ at $x=a$ may be obtained as

$$\begin{aligned} k(b) &= \lim_{x\to b} \sqrt{2(b-x)}\, \sigma_{yy}(x,0) \\ &= -\frac{4\mu}{1+\kappa} \lim_{x\to b} \sqrt{2(b-x)}\, \psi(x) \quad , \end{aligned} \tag{68}$$

$$\begin{aligned} k(a) &= \lim_{x\to a} \sqrt{2(x-a)}\, \sigma_{yy}(x,0) \\ &= \frac{4\mu}{1+\kappa} \lim_{x\to a} \sqrt{2(x-a)}\, \psi(x) \quad . \end{aligned} \tag{69}$$

Figure 2 shows some sample results for the crack surface displacement which is obtained from

$$v(x,0) = -\int_a^b \psi(t)dt \quad , \quad a<x<b \quad , \tag{70}$$

The contact stress distribution for various values b/h and a/h is shown in Figure 3. In this figure the stress $\sigma_{yy}(x,0)$ is normalized with respect to the average contact stress σ_0 given by

$$\sigma_0 = \frac{1}{a}\int_0^a \sigma_{yy}(x,0)dx \quad . \tag{71}$$

The stress $\sigma_{yy}(x,0)$ is obtained from (10) which is valid for $0<x<\infty$. The corresponding stress intensity factors are shown in Table 1 which also shows the resultant compressive wedging force per unit thickness calculated from

$$P_y = \int_0^a \sigma_{yy}(x,0)dx = a\sigma_0 \quad . \tag{72}$$

TABLE 1
Stress Intensity Factor for a Flat Wedge: $v_0/h = 0.1$

b/h	a/h	$\frac{1+\kappa}{4\mu h} P_y \cdot 10^2$	$\frac{k(b)}{P_y \cdot b/h^{3/2}}$
1.0	0.1	1.60	5.928
1.0	0.2	1.86	5.983
1.0	0.3	2.13	6.051
1.0	0.37	2.35	6.149
2.0	0.1	0.494	4.670
3.0	0.1	0.209	4.272
4.0	0.1	0.107	4.055

From Figure 3 it may be observed that for a fixed wedge thickness $2v_0$ and fixed crack length b, as penetration distance a increases the contact stress $\sigma_{yy}(x,0)$ at $x = 0$ decreases, and at a certain value of $a = a_1$ it becomes zero. For $a>a_1$ the procedure described above to solve the problem is not valid and the problem must be formulated in terms of a system of three integral equations as indicated by (17-19). In the example shown by Figure 3, $v_0 = 0.1h$, $b = h$, and the value a_1, at which the wedge starts separating from the strip is found to be $a_1 \cong 0.37b$.

As a second example we consider loading through a rigid frictionless wedge with a constant slope (see the insert in Figure 4). In this case the crack surface tractions $\sigma_{yy}(x,0)$, $a<x<b$, and $\sigma_{xx}(0,y)$, $0<y<h$, are again zero and the integral equations become (see equations (9) and (10))

$$\int_0^h H_{11}(y,r)\phi(r)dr + \int_a^b H_{12}(y,t)\psi(t)dt = 0 \quad , \quad 0<y<h \quad , \tag{73}$$

$$\int_0^h H_{21}(x,r)\phi(r)dr + \int_a^b H_{22}(x,t)\psi(t)dt = - \int_0^a H_{22}(x,t)f(t)dt \quad ,$$

$$a<x<b \quad , \tag{74}$$

where

$$f(x) = \frac{\partial}{\partial x} v(x,+0) = -f_0 \quad , \quad 0<x<a \quad . \tag{75}$$

Because of the smooth contact at $x = a$, the density function $\psi(x)$ is of the following form

$$\psi(x) = -f_0 + G(x)[(x-a)/(b-x)]^{1/2} \quad . \tag{76}$$

In solving the integral equations numerically we also modify the definition of $\phi(r)$ as

$$\phi(r) = \phi(h-\rho) = \phi_0(\rho) = f_0 + g(\rho)(h^2-\rho^2)^{1/2} \quad , \tag{77}$$

Note that with (76) and (77) the condition (58) is automatically satisfied.

In this problem the known loading parameter is either the wedge driving force P_0 or the wedge thickness δ at the strip end, i.e., $2v(0,0)$. The wedge thickness is calculated from

$$\delta = 2v(0,0) = 2(af_0 - \int_a^b \psi(t)dt) \quad . \tag{78}$$

Equations (71) and (72) are still valid giving the average contact stress σ_0 and the wedging force P_y, respectively. Once P_y is found, the wedge driving force may be obtained from

$$P_0 = 2P_y \sin(\tan^{-1} f_0) \simeq 2P_y f_0 \quad . \tag{79}$$

In this problem the contact distance a is unknown and is determined either from the equilibrium condition (72) or from (78). However, the problem is more conveniently solved by specifying a, solving the integral equations, and then determining the corresponding load P_0 or the thickness δ. Note that in this smooth contact problem the index of the integral equation (10) is zero and therefore no additional condition is required for a unique solution.

For a fixed crack length $b = h$ and wedge slope, $f_0 = 0.01$, Figure 4 shows the calculated values of the stress intensity factor as a function of δ, the crack opening at $x = 0$. Figure 5 shows a sample result for the distribution of the contact stress, σ_{yy} which is again normalized with respect to the average stress σ_0 given by (71). Figure 6 shows the crack surface displacement for various values of the crack length. Note that in order to have the same contact distance $a = 0.1h$, in a long crack the penetration of the wedge (or the crack opening at $x = 0$) needs to be much greater than that needed for a short crack.

The calculated stress intensity factors for a rigid wedge with a constant slope f_0 are summarized in Table 2. As indicated before, in the numerical analysis the contact distance a is specified and then the corresponding values $\delta = 2v(0,0)$ and the loads (per unit thickness) P_y and P_0 are calculated. The stress intensity factor $k(b)$ defined by (68) is shown in the last column. The particular normalization factor is introduced in order to compare the results with that of Ref. [2] and the beam theory. This comparison is shown in Figure 7. Using the classical beam theory, simple energy balance consideration would give the stress intensity factor as follows:

$$k(b) = \sqrt{12}\, P_y b/h^{3/2} \tag{80}$$

where P_y is a concentrated wedging force (per unit thickness) applied at the end $x = 0$. If the strain energy due to shear deformations is also taken into account, (80) is slightly modified and becomes

$$k(b) = \sqrt{12}\, (P_y b/h^{3/2})\left(1 + \frac{1+\nu}{5}\frac{h^2}{b^2}\right)^{1/2} . \tag{81}$$

TABLE 2

Stress Intensity Factor for a Rigid Wedge with Constant Slope

b/h	a/h	f_o	$\frac{\delta}{h}\,10^2$	$\frac{(1+\kappa)P_y}{4\mu h}\,10^3$	$\frac{(1+\kappa)P_o}{4\mu h}\,10^5$	$\frac{k(b)}{P_y \cdot b/h^{3/2}}$
1.0	0.05	0.01	0.597	1.31	2.62	5.918
1.0	0.1	0.01	1.078	2.53	5.05	5.926
1.0	0.15	0.01	1.458	3.57	7.14	5.943
1.0	0.2	0.01	1.735	4.38	8.77	5.950
1.0	0.4	0.01	2.166	5.84	11.7	6.065
1.0	0.1	0.04	4.314	1.01	80.8	5.926
2.0	0.1	0.01	2.838	2.31	4.62	4.597
3.0	0.1	0.01	5.791	2.12	4.23	4.150
4.0	0.1	0.01	9.962	1.94	3.88	3.912
5.0	0.1	0.01	15.33	1.79	3.58	3.715

Figure 7 shows the results obtained from the wedge solution (with $a = 0.1h$), Ref. [2], (80), and (81). The results given in [2] were calculated by using a boundary collocation method for a strip which has a finite length. Considering the differences in loading and geometry the agreement is reasonable.

Finally, a sample result for the crack opening displacement in a strip subjected to a distributed wedge force is shown in Figure 8. Here the crack surface traction is assumed to be

$$\sigma_{yy}(x,+0) = -\frac{p_o}{h}\sqrt{d^2-(x-D)^2} \quad . \tag{82}$$

This is an elliptic distribution which may be representative of smooth contact problems with elastic wedges. In the example the constants are assumed to be

$$b = 1.143h \quad , \quad D = 0.524h \quad , \quad d = 0.2h \quad . \tag{83}$$

The b/h ratio considered here corresponds to the standard compact tension specimen. For this example the stress intensity factor is found as

$$\frac{k(b)}{P_y b/h^{3/2}} = 5.971 \quad , \quad p_0 = \frac{2}{\pi}\frac{h}{d^2}P_y \quad , \tag{84}$$

where P_y is the resultant force per unit thickness.

Using the analysis given in this paper one may easily calculate a "Green's function" for the stress intensity factor k(b) which can be used to solve the edge crack problem under an arbitrarily distributed crack surface pressure. To do this in (9) and (10) we substitute $c = 0$, $d = h$, $\sigma_{xx} = (0,y)$ and assume that

$$\sigma_{yy}(x,0) = \begin{cases} -1 \text{ for } x = x_i \quad , \\ 0 \text{ for } x = x_j, \; j = 1,..,i-1, \; i+1,..,n \end{cases} \tag{85}$$

where x_i/b, $i = 1,..,n$ are the appropriate collocation points in (0,1) used in the solution of the singular integral equations. Solving the problem for the loading (85) the stress intensity factor is obtained as a function of x_i in the following form:

$$k(b,x_i) = G(x_i) \quad , \quad i = 1,..,n \quad . \tag{86}$$

If the crack surface pressure is now specified as

$$\sigma_{yy}(x,0) = -f(x) \quad , \quad 0<x<b \quad , \tag{87}$$

then the stress intensity factor may be obtained as follows:

$$k(b) = \sum_{i=1}^{n} G(x_i)f(x_i) \quad . \tag{88}$$

This procedure follows from the method of solution used in solving the singular integral equations. It may be noted that $G(x_i)$ also corresponds to the stress intensity factor due to a concentrated wedging force of unit magnitude applied at $x = x_i$. Table 3 shows an example obtained for $b = h$.

TABLE 3
Green's Function for a Symmetric Crack in a Semi-infinite Strip, b = h

i	x_i/b	$G(x_i)/(b/h^{3/2})$
1	0.001	5.915
2	0.013	5.919
3	0.036	5.923
4	0.070	5.930
5	0.114	5.951
6	0.167	5.986
7	0.228	6.063
8	0.295	6.169
9	0.368	6.329
10	0.443	6.495
11	0.519	6.690
12	0.595	7.009
13	0.669	7.400
14	0.739	8.092
15	0.803	9.050
16	0.860	10.416
17	0.909	12.13
18	0.948	15.75
19	0.977	23.31
20	0.994	44.95

References

1. O. L. Bowie, Methods of Analysis and Solutions of Crack Problems, G. C. Sih, ed., Noordhoff Int. Publ. Leyden (1973).

2. B. Gross and J. E. Srawley, "Stress Intensity Factors by Boundary Collocation for Single-Edge-Notch Specimens Subject to Splitting Forces", NASA TND-3295 (1966).

3. J. C. Newman, Jr., "An Improved Method of Collocation for the Stress Analysis of Cracked Plates with Various Shaped Boundaries", NASA TN D-6376, Langley Research Center (1971).

4. W. K. Wilson, "Finite Element Methods for Elastic Bodies Containing Cracks", in Methods of Solutions of Crack Problems, G. C. Sih, ed., Noordhoff Int. Publ., Leyden (1973).

5. F. Erdogan and K. Arin, "Fracture and Contact Problems for an Elastic Wedge", Journal of Elasticity, Vol. 6, 1976, pp. 57-71.

6. F. Erdogan and K. Arin, "Effect of Friction in Wedging of Elastic Solids", Journal of Elasticity, Vol. 6, 1976, pp. 261-275.

7. I. N. Sneddon and M. Lowengrub, Crack Problems in the Classical Theory of Elasticity, John Wiley & Sons, New York (1969).

8. G. D. Gupta and F. Erdogan, "The Problem of Edge Cracks in an Infinite Strip", J. Appl. Mech., Vol. 41, Trans. ASME, 1974, pp. 1001-1006.

9. F. Erdogan and G. D. Gupta, "On the Numerical Solution of Singular Integral Equations", Q. Appl. Math., Vol. 30, 1972, pp. 525-534.

10. A. Erdelyi, ed., Tables of Integral Transforms, Vol. 1, McGraw-Hill, New York (1953).

11. N. I. Muskhelishvili, Singular Integral Equations, Noordhoff, Groningen, the Netherlands (1953).

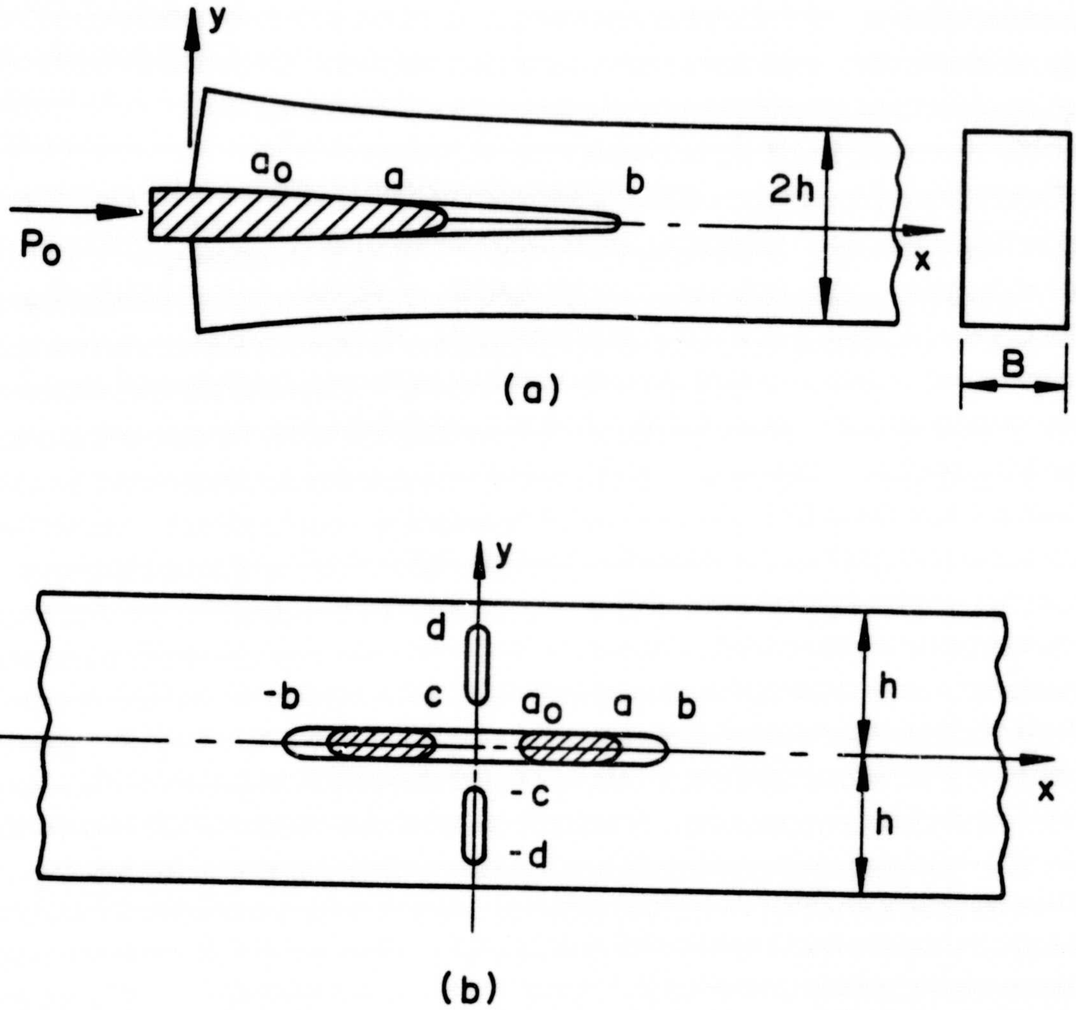

Figure 1 Geometry of the cracked strip

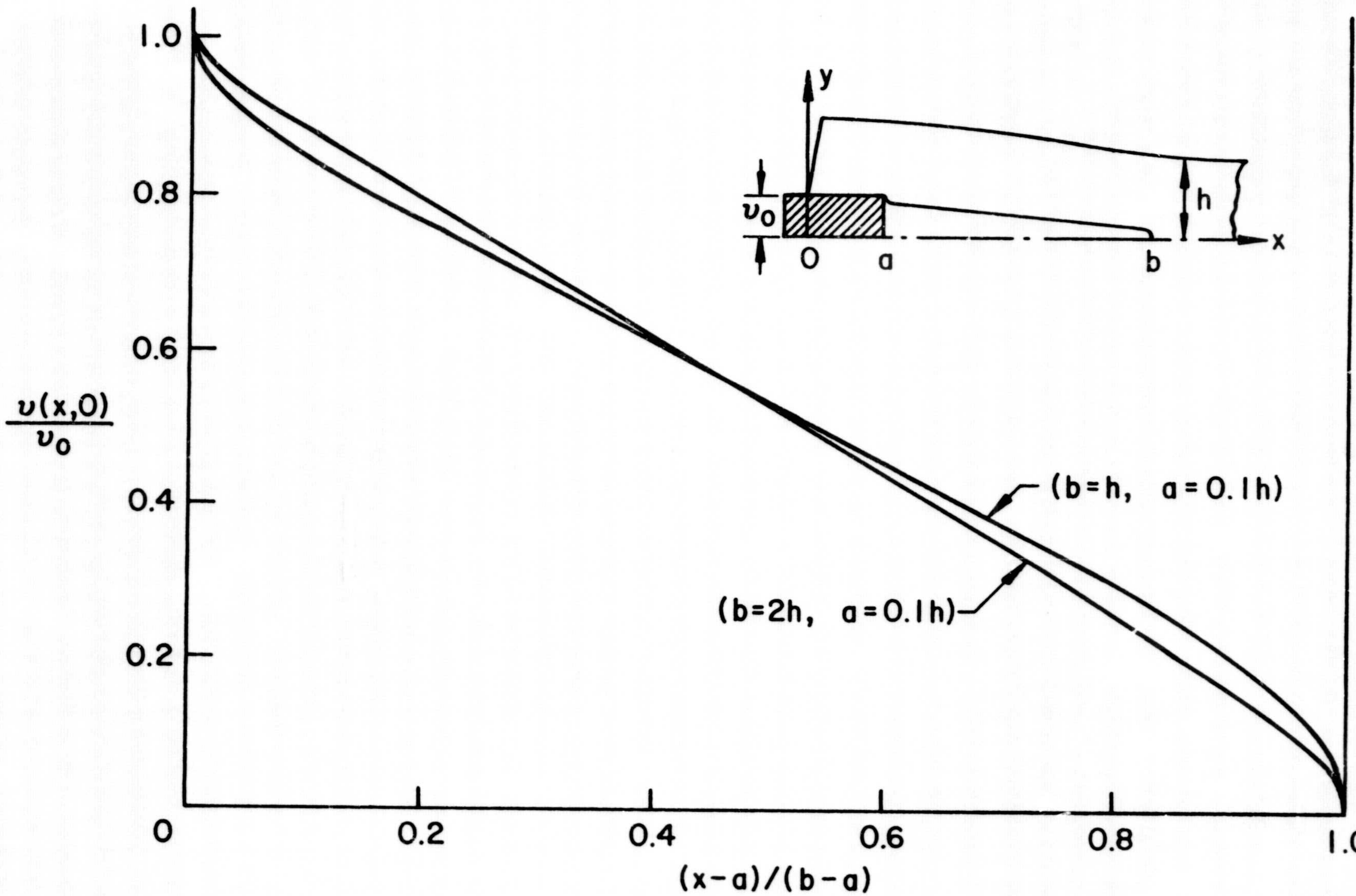

Figure 2 Crack surface displacement in a strip loaded by a flat wedge, $v_0 = 0.1h$

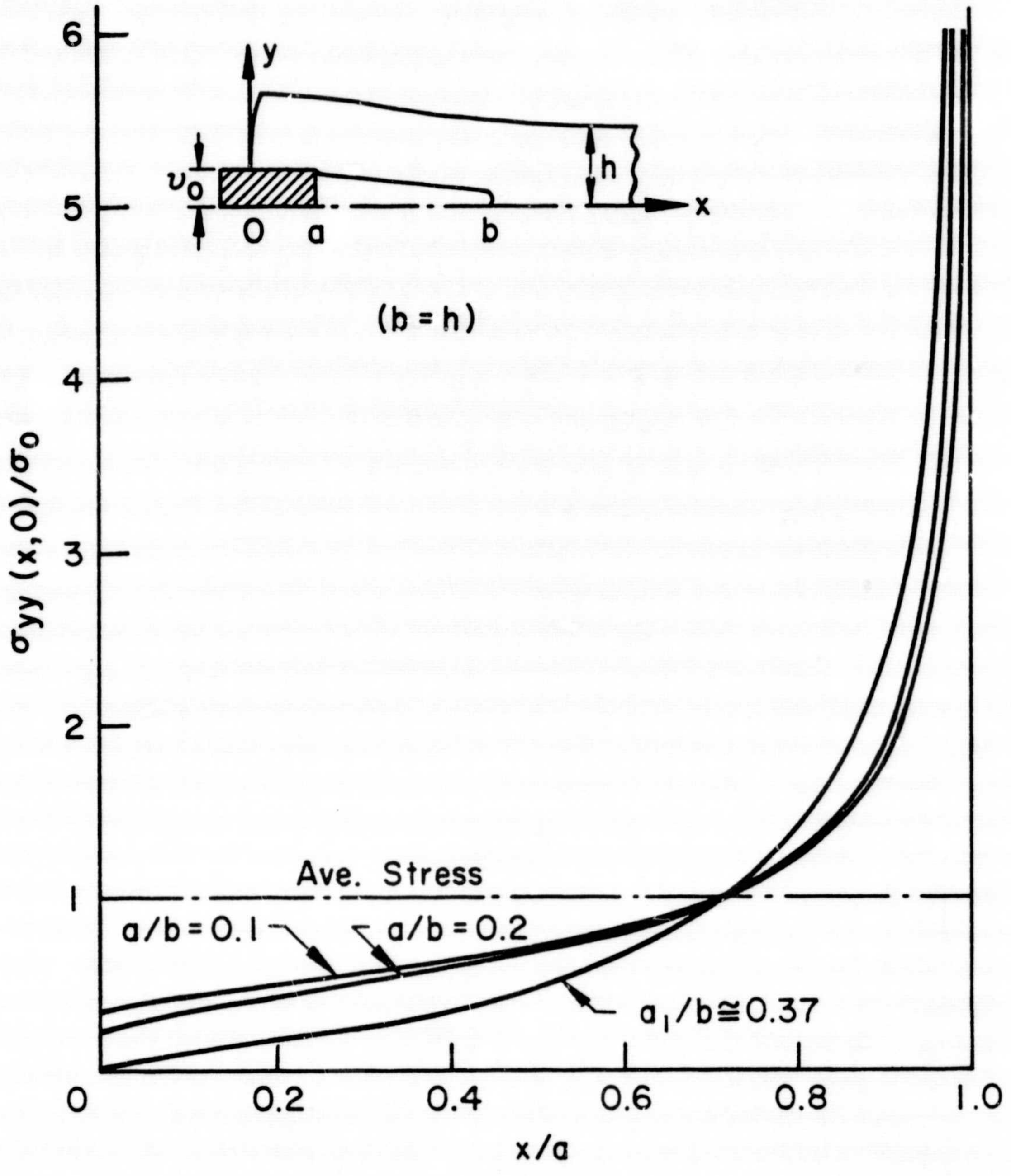

Figure 3 Distribution of the contact stress in a strip loaded by a flat wedge, $b = h$, $v_0 = 0.1h$

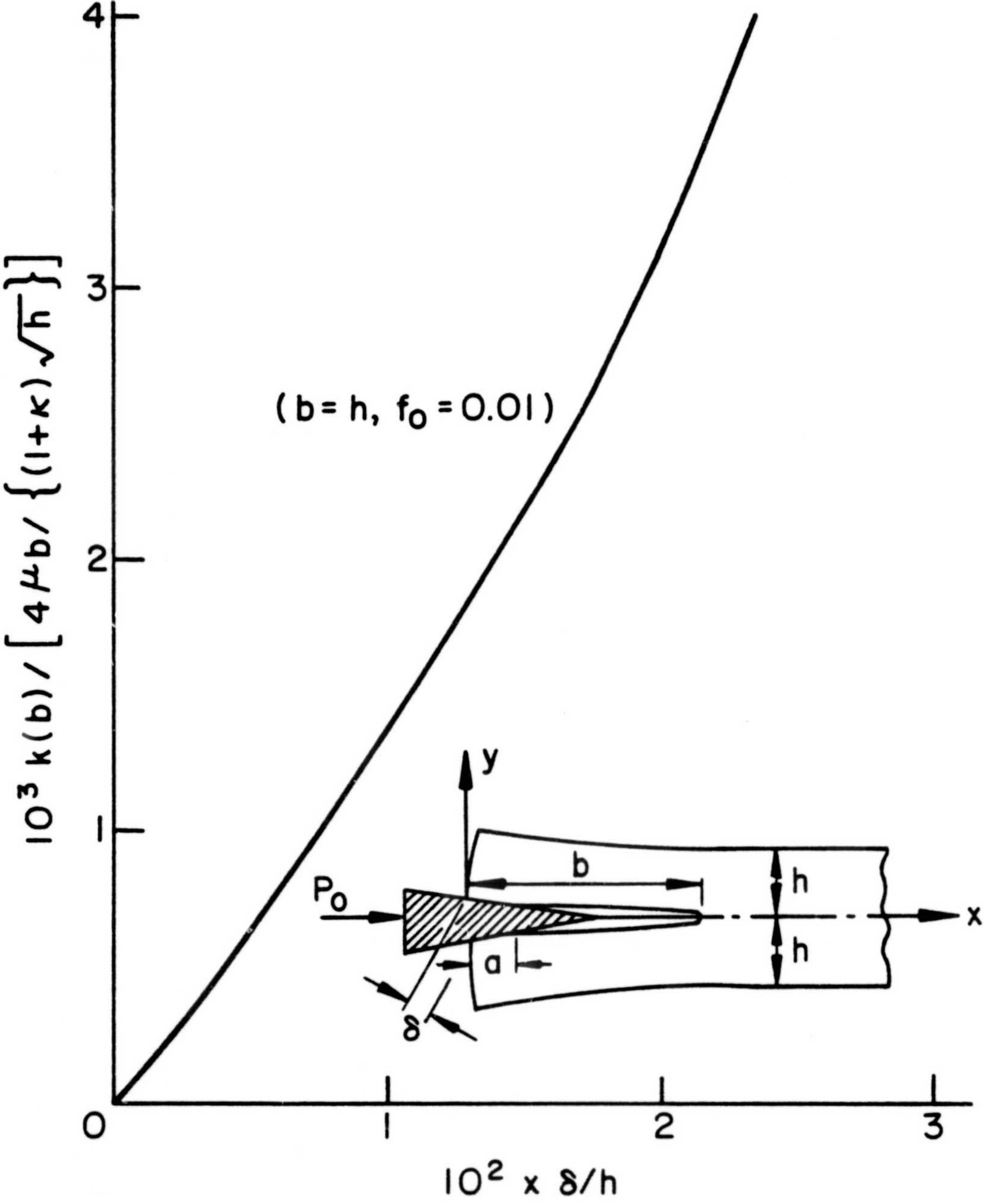

Figure 4 Stress intensity factor in a strip loaded by a rigid wedge with constant slope. $\partial v(x,+0)/\partial x = -f_0 = -0.01$, $b = h$, $\delta = 2v(0,0)$ (crack opening at $x = 0$)

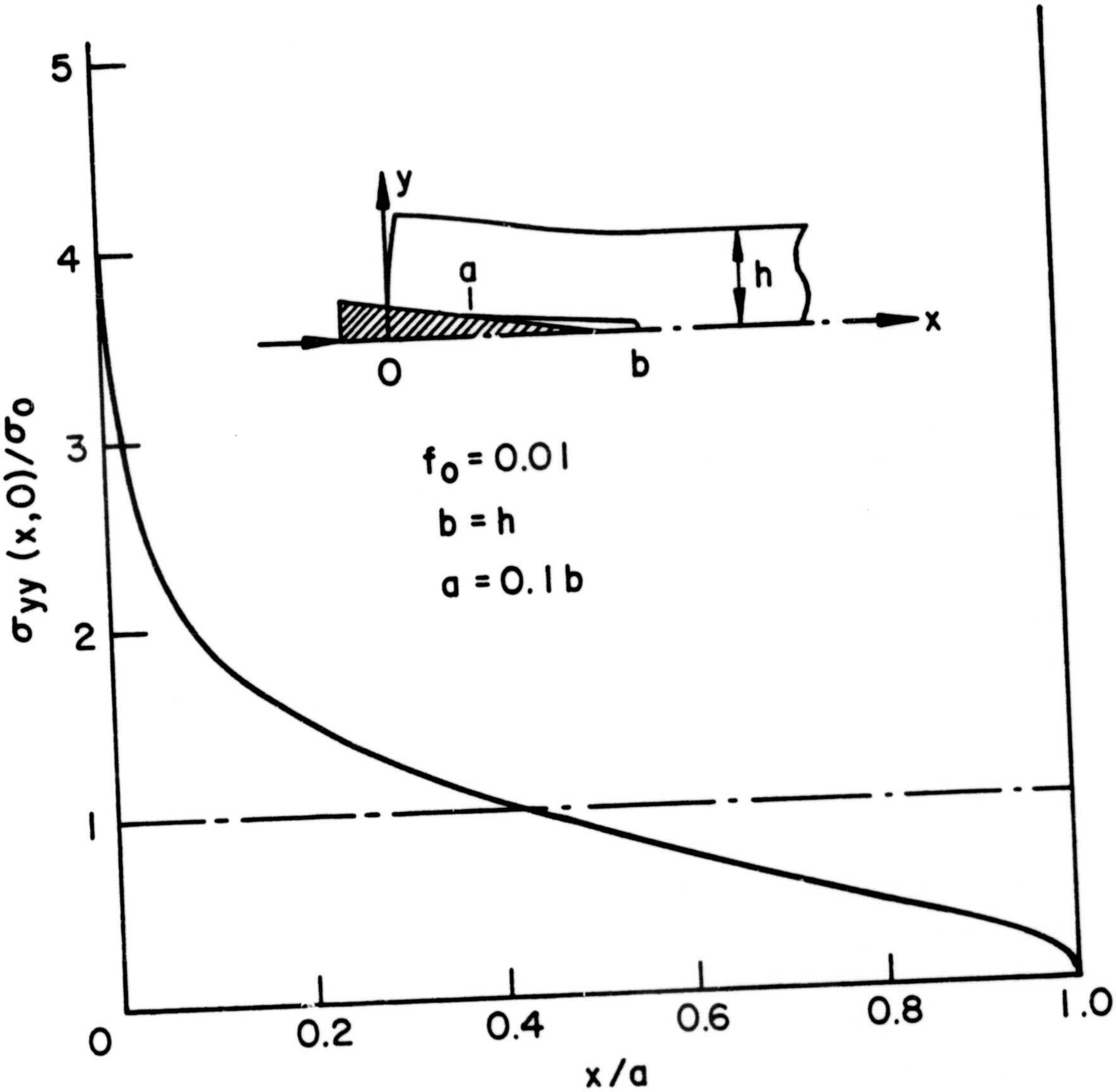

Figure 5 Contact stress distribution for a wedge with constant slope. $f_o = 0.01$, $b = h$, $a = 0.1b$

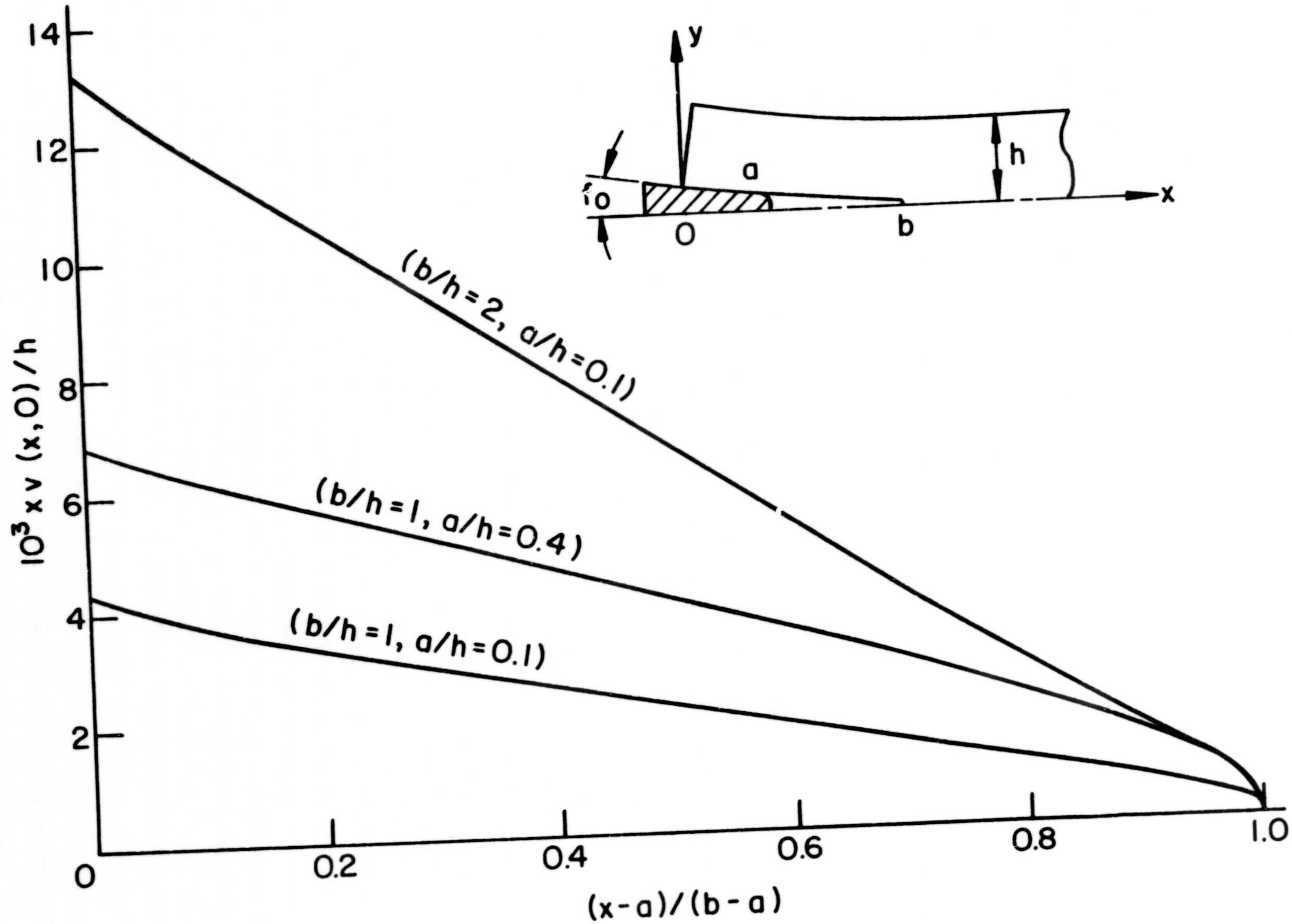

Figure 6 Crack surface displacement in a strip loaded by a wedge with constant slope, $f_0 = 0.01$

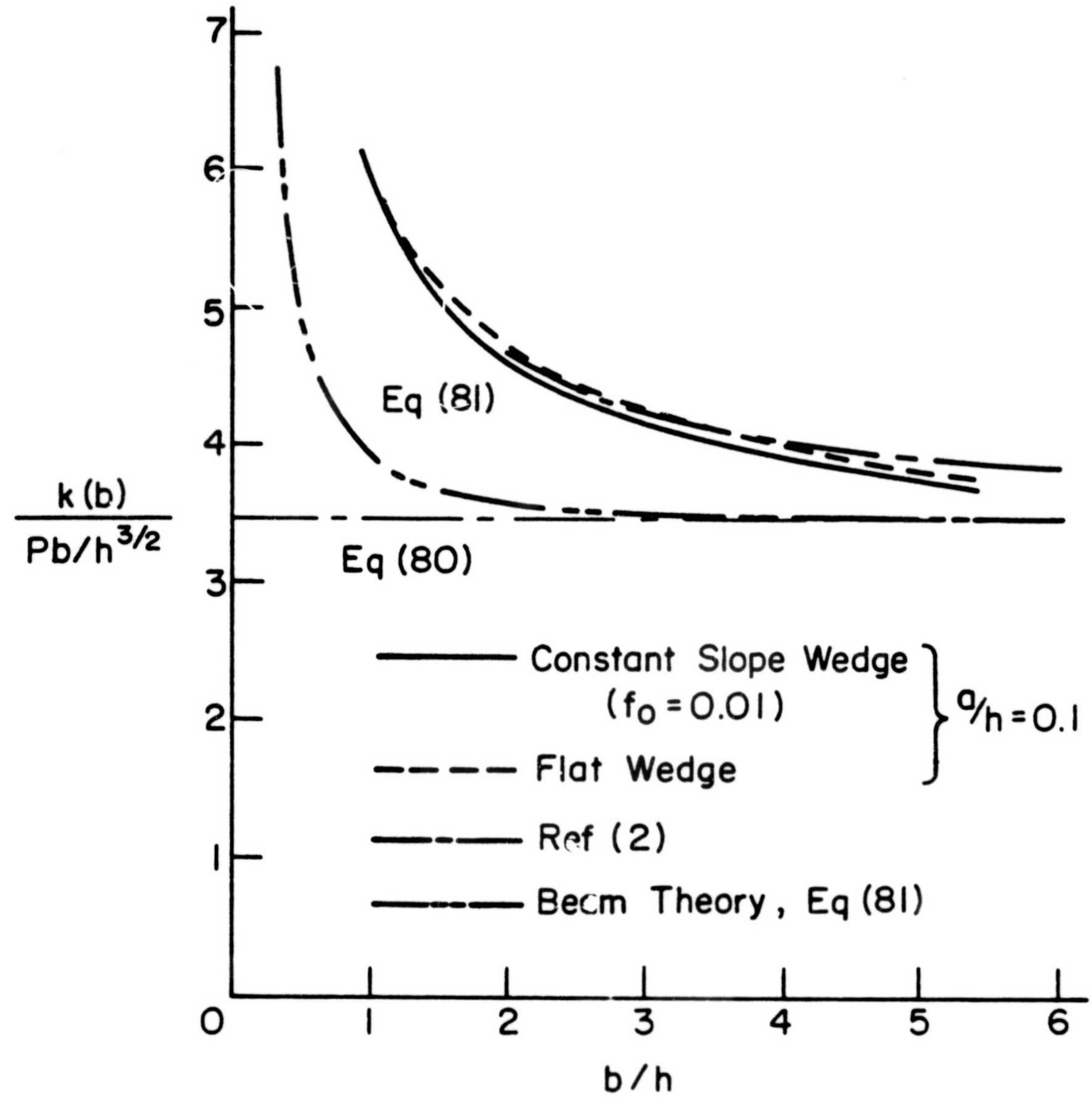

Figure 7 Stress intensity factor in a strip loaded by a wedge with constant slope, $f_0 = 0.01$, $a = 0.1h$

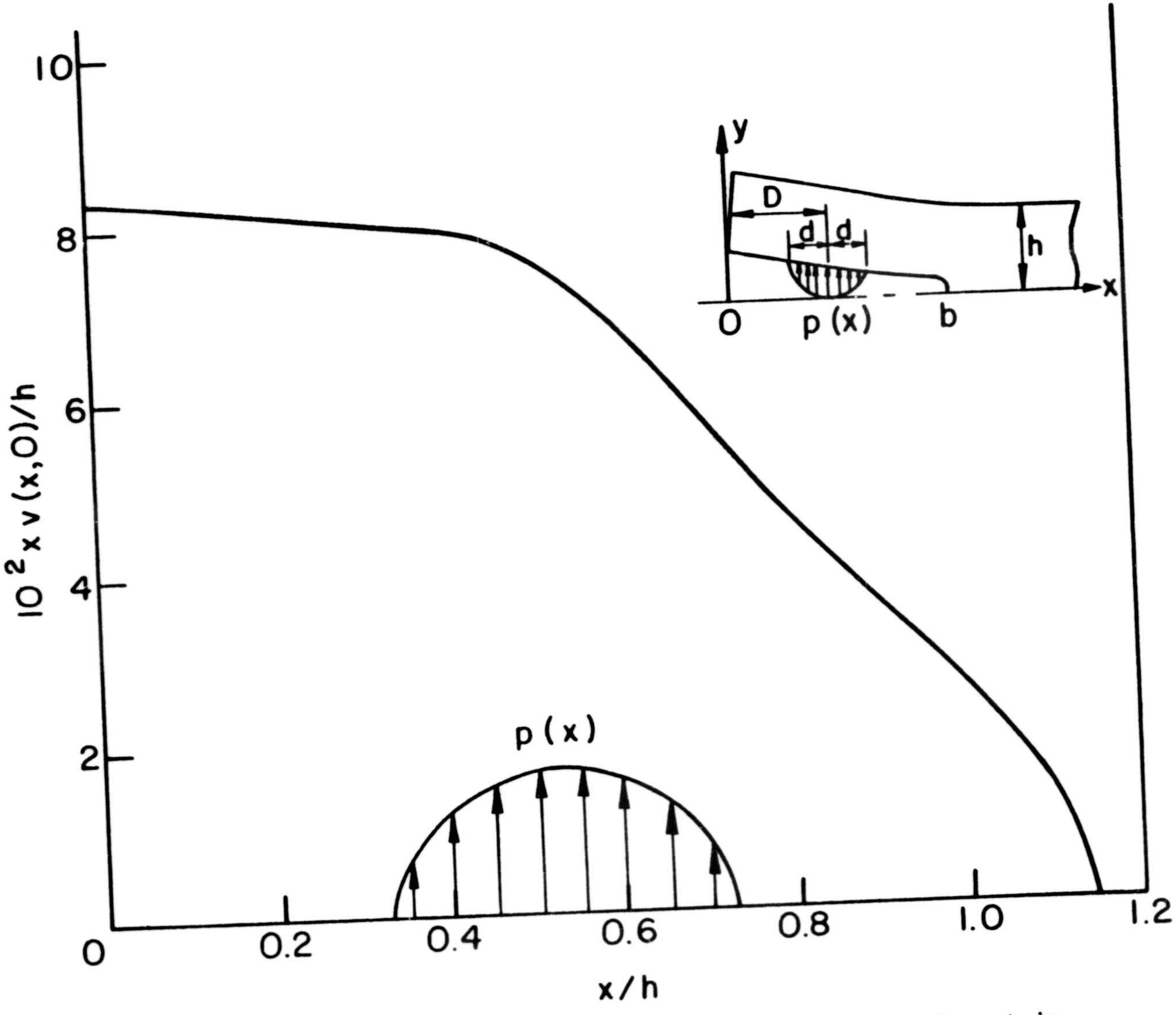

Figure 8 Crack surface displacement in a semi-infinite strip wedge-loaded by pressure of elliptic profile